

Lasers in Manufacturing Conference 2021

Theoretical analysis of the incubation effect on the ablation behavior using spatial shaped ultra-short pulse laser

Marco Smarra^{a,*}, Cemal Esen^a, Andreas Ostendorf^a, Evgeny Gurevich^b

^aApplied Laser Technologies, Ruhr University Bochum, Universitätsstraße 150, 44801 Bochum, Germany

^bLaser Center of the University of Applied Sciences Muenster, Stegerwaldstr. 39, 48565 Steinfurt, Germany

Abstract

Ultra-short laser pulses are well known for their low thermal effect on the ablation process and therefore are used in numerous applications like surface texturing and functionalization. However, high peak fluence can lead to a reduction in ablation efficiency. Beam shaping can be used to solve this issue. Beam errors, like defocus or astigmatism, lead to a larger beam radius and a decrease of the fluence on the surface of the workpiece. This paper focuses on the theoretical study of the incubation effect and its influences on the ablated volume per pulse by analyzing the effects of the waist position of the laser beam and the ablation threshold of the sample material. This work is fundamental for handling the ablation process using high pulse energies.

Keywords: Laser Ablation; Laser Beam Shaping; Laser Micro Processing; Ultra-Short Laser Pulses

1. Introduction

Ultra-short laser pulses are used in a wide range of microprocessing applications, such as cutting, drilling, structuring, or even welding. The main feature using the short interaction time between the pulse energy and the material is the low thermal effects causing damage or stress. The ablation process depends on beam properties, like pulse energy and spot size, and material properties, like the ablation threshold (F_{th}) and absorption depth of the laser energy (δ). The ablation threshold can be measured using the squared diameter of small craters produced at several pulse energies (Barthels and Reininghaus 2018; Liu 1982; Bonse et al. 2000). Besides, the number of pulses (N) interacting with the surface or the already produced crater influences the ablation threshold. This effect is called the incubation effect (Liu 1982; Ashkenasi et al.

* Corresponding author. E-mail address: smarra@lat.rub.de

2000; Di Niso et al. 2013; Jee et al. 1988; Mannion et al. 2004). It is described by the accumulation factor S , who is material-specific and ranging between $[0; 1]$.

$$F_{th,N} = F_{th,1} \cdot N^{S-1} \quad \text{Eq. 1}$$

Laser energy hitting the surface of a material can be absorbed. The depth of the absorption of the laser energy depends on the material-specific absorption length (δ), which results from the Lambert-Beer absorption law. Knowing the threshold fluence of the material and the fluence on the surface (F_w), the ablation depth per pulse (L_{pulse}) can be calculated (Nolte et al. 1997). Its logarithmic increase conquers the increasing pulse energies of current laser developments.

$$L_{pulse} \propto \delta \cdot \ln \frac{F_w}{F_{th}} \quad \text{Eq. 2}$$

Depending on the beam properties, the radius of the laser spot $w(z)$ increases when leaving the waist (w_0). With the increase of the radius, the fluence of the beam decreases. By increasing the distance between waist and workpiece surface (defocus), the interacting beam radius (w_{eff}) shows a double-lobe structure. The width and length of each lobe depend on the laser's pulse energy and beam properties and the ablation threshold fluence of the material (Chang et al. 2012; Luzius et al. 2012;). The interacting beam radius can be characterized by

$$w_{eff} = w(z) \cdot \sqrt{-\frac{1}{2} \ln \left(\frac{F_{th}}{F_0} \cdot \left(\frac{w(z)}{w_0} \right)^2 \right)} \quad \text{Eq. 3}$$

Here (F_0) is the peak fluence in the waist of the laser beam. The interacting beam radius is derived by the intensity distribution along with the propagation, the ablation threshold intensity necessary for the ablation process, and the spot size along with its propagation

$$w(z) = w_0 \sqrt{1 + \left(\frac{z - z_0}{z_R} \right)^2} \quad \text{Eq. 4}$$

First experimental results by (Chang et al. 2012; Luzius et al. 2012; Smarra and Dickmann 2015a, 2015b; Smarra et al. 2016) demonstrate the influence of the defocus for a single pulse and volume ablation. In this paper, the incubation effect and the interacting diameter are combined to simulate the theoretical influence on the ablation process when changing the beam shape on the workpiece surface, e.g., by increasing the distance between the waist and workpiece surface.

2. Simulation

For the simulation of the influence of the incubation effect, an arbitrary Gaussian beam with a waist radius of $w_0 = 12.5 \mu\text{m}$ and a Rayleigh length of $z_R = 250 \mu\text{m}$ is used. These were typical values, using a wavelength of $\lambda = 1030 \text{ nm}$ and an f-theta lens with a focal length of $f_\theta = 100 \text{ mm}$. Fig. 1 demonstrates the definitions used in this section: The *defocus* describes the waist position (z_0) referred to the work piece surface. By the *spot size*, the beam radius on the workpiece surface (defined by the intensity decrease to I_0/e^2) is described. Finally, the *effective beam radius* is the part of the beam interacting with the workpiece surface, where the fluence is above the ablation threshold fluence.

Fig. 2 (blue) shows the relative spot size ($w(z)/w_0$) and the relative fluence on the workpiece ($F_w(z_0)/F_w(z_0 = 0)$) in dependence on the waist position (z_0) referred to the workpiece surface. Increasing the defocus, the spot size increases: A defocus of e.g. $z_0 = 2$ mm, the spot size increases by a factor of 8.

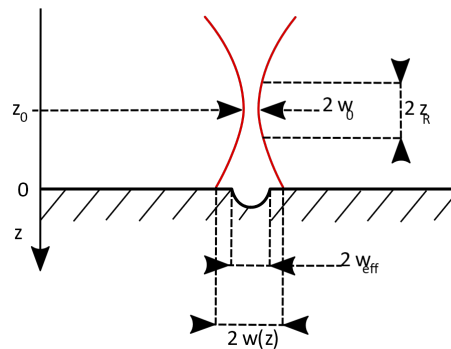


Fig. 1: Definition of beam parameters.

The spot size determines the fluence on the workpiece surface (for constant pulse energy, here $E_p = 10 \mu\text{J}$). Thus, an increasing defocus leads to a decreasing fluence on the workpiece, as shown in Fig. 2. The decrease depends on the Rayleigh length, as the increase of the spot size also depends on the Rayleigh length: The longer the Rayleigh length, the lower the decrease of the fluence on the workpiece.

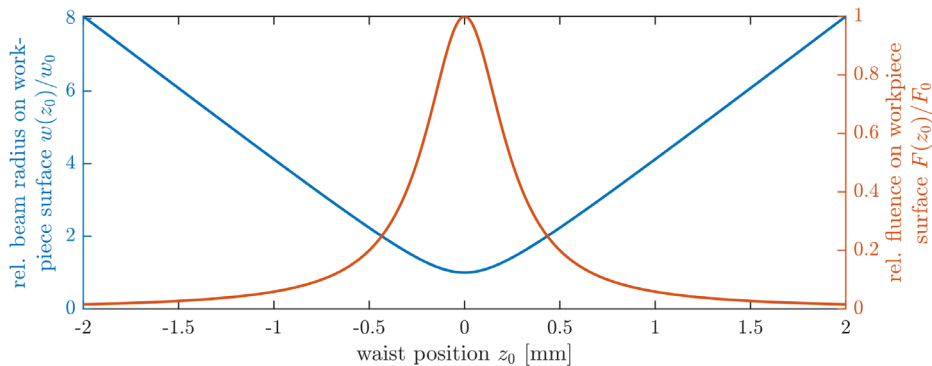


Fig. 2: Relative beam radius and fluence on the work piece surface in dependence on the waist position.

Most laser processes use a (relative) lateral movement between the laser beam and the workpiece. This simulation is based on the ablation of ultra-short pulse lasers. The laser beam movement influences the number of interacting pulses on the same infinitesimal small area of the workpiece surface. For a constant pulse to pulse distance (e.g., $dp_x = 5 \mu\text{m}$), the increasing spot size due to the increasing defocus, leads to a rising number of overlapping pulses. Here the number of interacting pulses is the ratio of the laser spot size and the pulse to pulse distance. For more detailed analysis, it would be necessary to determine the spot size on the workpiece surface, which again is a function of the threshold fluence. Fig. 3 (blue) shows this dependence. As a simplification, only the movement in one direction is analyzed. If the beam or workpiece is

moved in 2 perpendicular dimensions with the same pulse to pulse distance in each dimension, the number of interacting pulses must be squared.

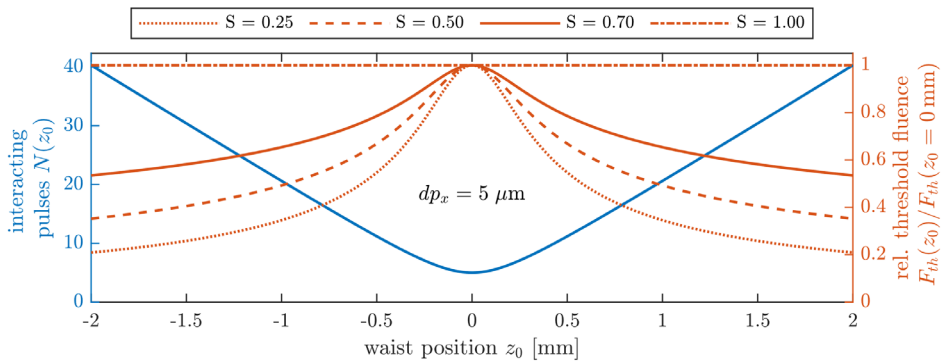


Fig. 3: Number of interacting pulses at an infinitesimal small area of the work piece and threshold fluence in relation to the threshold fluence for a waist on the work piece surface in dependence on the waist position.

The increasing number of interacting pulses leads to a decreased threshold fluence due to the incubation effect. Fig. 3(red) shows the dependence of the threshold fluence on the waist position. The threshold fluence is shown concerning the threshold fluence for the waist of the laser beam on the workpiece surface. An arbitrary threshold fluence of $F_{th,z=0} = 0.1 \text{ J/cm}^2$ is estimated for a single pulse ablation and the waist on the surface of the workpiece. Four arbitrary accumulation factors S are compared. Neglecting the incubation effect would result in a waist position-independent threshold fluence ($S = 1$). Considering the incubation effect and respecting the increasing number of interacting pulses by increasing the defocus, the threshold fluence is reduced. This reduction depends on the accumulation factor S . The more the value of the accumulation factor approaches one, the smaller the reduction of the threshold fluence. A higher accumulation factor leads to a higher threshold fluence at the same defocus.

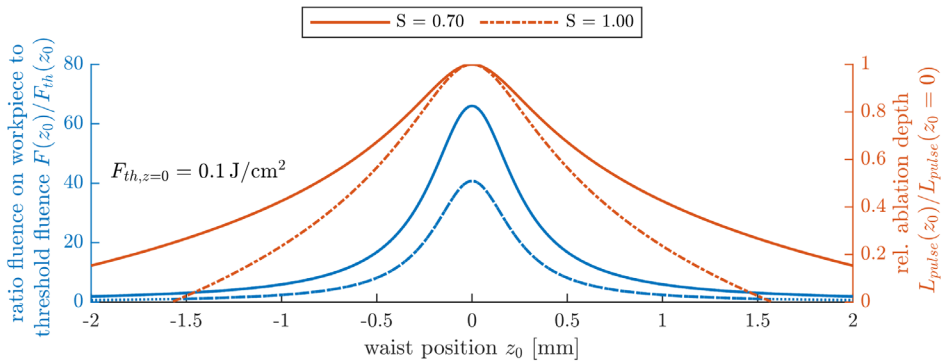


Fig. 4: Ratio workpiece fluence to threshold fluence and rel. ablation depth per pulse in dependence on the waist position.

The ablation depth of a laser pulse depends on the penetration depth of the energy (δ) and the logarithmic ratio of the peak (F_0) to the threshold fluence (F_{th}), see Eq. 2. Hence from the fluence on the workpiece (equals the peak fluence in Eq. 2) in dependence of the waist position (Fig. 2) and the threshold fluence in dependence of the waist position (Fig. 3, blue), the ratio of the peak to the threshold fluence can

be calculated (see Fig. 4, blue). Here the accumulation factors $S = 0.7$ and $S = 1.0$ were used. The highest ratio can be achieved for the waist of the laser beam on the workpiece sample. By increasing the defocus, the ratio decreases. The lower the accumulation factor, the slighter the decrease of the aspect ratio. The lower the accumulation factor is, the higher the fluence ratio (fluence on workpiece surface to threshold fluence) at the same waist position. For the ablation depth per pulse, see Eq. 2. It is relevant that the fluence ratio on the workpiece to the threshold fluence is greater than 1. Otherwise, the ablation stops, indicated by the dotted lines of the fluence ratio.

For a constant penetration depth (e.g., $\delta = 10$ nm) and fluence ratio, the ablation depth per pulse can be calculated, see Fig. 4 (red): The ablation depth per pulse in relation to the ablation depth for the waist on the workpiece surface is shown in dependence on the waist position. The larger the defocus, the lower the ablation depth per pulse. When the fluence ratio reaches 1, the ablation depth is 0. Here again, the lower the accumulation factor, the lower the slope of the ablation depth per pulse for an increasing defocus.

The effective beam radius depending on the waist position can be calculated from the fluence ratio following Eq. 3. Fig. 5 (blue) demonstrates the effective beam radius on the workpiece surface related to the waist radius (on the workpiece surface) depending on the waist position. Two arbitrary accumulation factors are shown: $S = 0.7$ (solid line) and $S = 1.0$ (dashed line)

The interacting beam radius increases from a waist on the workpiece surface and increasing the defocus. This increase depends on the accumulation factor (S). The lower the accumulation factor, the higher the increase. This increase is due to the increasing beam radius. As long as the fluence of the beam is higher than the ablation threshold fluence, the beam interacts with the workpiece surface by ablating material. By further defocusing, a maximum of the interacting beam radius can be reached. Again, this maximum also depends on the accumulation factor. After this maximum, the interacting beam radius rapidly drops to zero when further increasing the defocus. The decrease is based on the decreasing fluence on the workpiece by increasing the beam radius. When increasing the defocus after the maximum of the interacting beam radius, the fluence on the workpiece is reduced. When the fluence on the workpiece is lower than the ablation threshold, so the ablation stops.

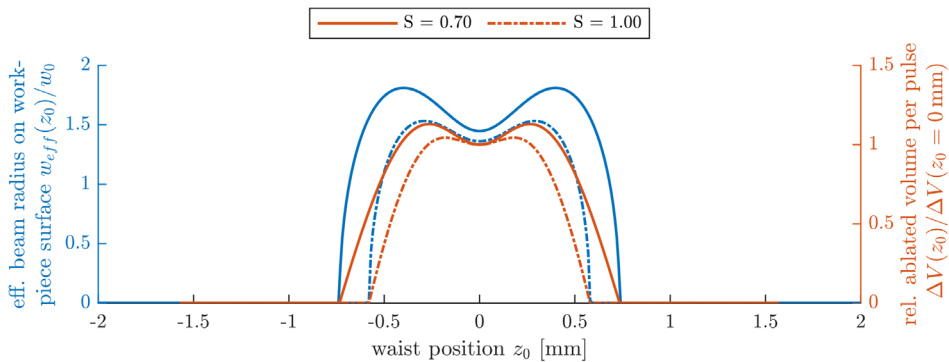


Fig. 5: Influence of the waist position on the ratio of the effective beam radius to the waist radius on the workpiece surface and the ratio of the ablated volume per pulse to the ablated volume per pulse for a waist on the workpiece surface.

Taking into account the interacting radius is in the range of a few ten to hundred micrometers and the ablation depth per pulse is in the range of a few nanometers, a cylinder volume can estimate the ablated volume per pulse $V_{cyl} = \pi r^2 \cdot h$. Here, the radius (r) is equal to the interacting beam radius (w_{eff}) and the height (h) of the cylinder is the ablation depth per pulse (L_{pulse}). With this estimation, the ablated volume per pulse depending on the waist position related to the workpiece surface can be calculated, see Fig. 5

(red). The ablated volume per pulse related to the ablated volume per pulse for the waist on the workpiece surface is shown. As shown for the interacting beam radius, the ablated volume per pulse increases to a maximum by increasing the defocus. The increase depends on the accumulation factor. The lower the accumulation factor, the higher the increase. The maximum of the ablated volume per pulse and the maximum of the interacting beam radius is not located at the same waist position. The maximum of the ablated volume is located between the maximum of the interacting waist radius and the workpiece surface. The value of the ablated volume per pulse also depends on the accumulation factor. Neglecting the incubation effect, by $S = 1.0$, increasing the defocus to about $z_0 = \pm 0.3$ mm, increases the ablated volume per pulse by about 20 %. The maximum of the ablated volume per pulse for an accumulation factor of $S = 0.7$ can be reached by a focus shift of $z_0 \approx \pm 0.4$ mm. Here the ablated volume per pulse increases by about 40 %. Reducing the ablated volume per pulse after the maximum is lower than the interacting waist radius. The ablated volume per pulse is 0 when the interacting beam radius is 0, too. Although the ablation depth per pulse seems to be dropping over a broader range of the focus shift.

So far, for the calculations constant pulse energy of $E_p = 10 \mu\text{J}$ and threshold fluence of $F_{th,z=0} = 0.1 \text{ J/cm}^2$ were used. It was shown that the focus shift could increase the ablated volume per pulse. The range of the focus shift resulting in an increase of the ablated volume per pulse compared to the waist on the workpiece surface is limited. It depends on the accumulation factor and the fluence ratio. The latter is shown for pulse energies up to $E_p = 100 \mu\text{J}$ in Fig. 6. Here, the relative ablated volume per pulse in dependence on the waist position is demonstrated for a constant threshold fluence ($F_{th,z=0} = 0.1 \text{ J/cm}^2$). For each pulse energy (y-axis), the ablated volume per pulse is related to the ablated volume per pulse for the waist on the workpiece surface $\Delta V(E_p, z_0 = 0 \text{ mm})$. In this way, it can be seen that by increasing the pulse energy, the ablated volume per pulse can increase by defocussing. The higher the pulse energy, the broader the range of the focus shift, maximizing the ablated volume per pulse. However, the optimal waist position for the maximum ablated volume per pulse does not increase linearly with the pulse energy. Besides, the increase of the maximal ablated volume per pulse does not increase linearly with the pulse energy, too.

This simulation does not include effects resulting from plasma or surface roughness nor the repetition

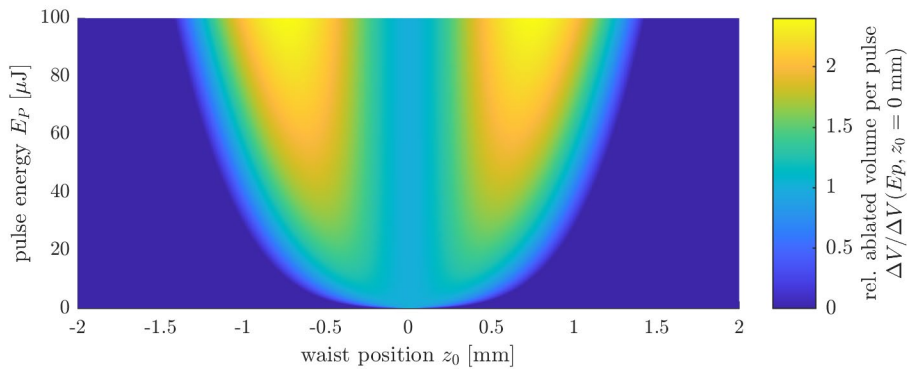


Fig. 6: Relative ablated volume per pulse in dependence on the waist position and the pulse energy. The ablated volume per pulse for each pulse energy is shown in relation to the ablated volume per pulse for the waist on the workpiece surface for each pulse energy.

rate. Nevertheless, concerning a constant repetition rate, the average power for each pulse energy is the same. So for high pulse energies, the efficiency of the ablation process increases by defocusing the beam.

3. Conclusion

In this paper, we demonstrate the influence of the waist position related to the workpiece surface on the ablated volume per pulse. Increasing the defocus leads to increasing spot size. The increasing spot size, on the one hand, reduces the fluence on the workpiece surface. On the other hand, the increasing spot size increases the number of interacting pulses on the same infinitesimal small material area. This increasing number of interacting pulses on the workpiece surface reduces the threshold fluence via the incubation effect. Depending on the accumulation factor, the maximal ablated volume per pulse can be achieved by increasing the defocus. Concerning the current developments of new ultra-short pulse lasers with respect to increasing pulse energies, the result of this work influence the design of ablation processes.

Acknowledgments

This work was part of the project “MOVERO” (‘Development of modern techniques for surface structuring with applications in the regional industry’) funded by the EU. It aimed to produce functional surface structures for large-area applications efficiently.

References

- Ashkenasi, D.; Stoian, R.; Rosenfeld, A. (2000): Single and multiple ultrashort laser pulse ablation threshold of Al₂O₃ (corundum) at different etch phases. In *Applied Surface Science* 154-155, pp. 40–46. DOI: 10.1016/S0169-4332(99)00433-X.
- Barthels, Thilo; Reininghaus, Martin (2018): High precision ultrashort pulsed laser drilling of thin metal foils by means of multibeam processing. In Angela Dudley, Alexander V. Laskin (Eds.): *Laser Beam Shaping XVIII*. Laser Beam Shaping XVIII. San Diego, United States, 19.08.2018 - 23.08.2018: SPIE, p. 10. Available online at <https://www.spiedigitallibrary.org/conference-proceedings-of-spie/10744/2320268/High-precision-ultrashort-pulsed-laser-drilling-of-thin-metal-foils/10.1117/12.2320268.full>.
- Bonse, J.; Rudolph, P.; Krüger, J.; Baudach, S.; Kautek, W. (2000): Femtosecond pulse laser processing of TiN on silicon. In *Applied Surface Science* 154-155, pp. 659–663. DOI: 10.1016/S0169-4332(99)00481-X.
- Chang, Gang; Tu, Yiliu (2012): The threshold intensity measurement in the femtosecond laser ablation by defocusing. In *Optics and Lasers in Engineering* 50 (5), pp. 767–771. DOI: 10.1016/j.optlaseng.2011.12.010.
- Di Niso, F.; Gaudiuso, C.; Sibillano, T.; Mezzapesa, F. P.; Ancona, A.; Lugarà, P. M. (2013): Influence of the Repetition Rate and Pulse Duration on the Incubation Effect in Multiple-Shots Ultrafast Laser Ablation of Steel. In *Physics Procedia* 41, pp. 698–707. DOI: 10.1016/j.phpro.2013.03.136.
- Jee, Yong; Becker, Michael F.; Walser, Rodger M. (1988): Laser-induced damage on single-crystal metal surfaces. In *J. Opt. Soc. Am. B* 5 (3), p. 648. DOI: 10.1364/JOSAB.5.000648.
- Liu, J. M. (1982): Simple technique for measurements of pulsed Gaussian-beam spot sizes. In *Opt. Lett.* 7 (5), p. 196. DOI: 10.1364/OL.7.000196.
- Mannion, P.T; Magee, J.; Coyne, E.; O’Connor, G.M; Glynn, T.J (2004): The effect of damage accumulation behaviour on ablation thresholds and damage morphology in ultrafast laser micro-machining of common metals in air. In *Applied Surface Science* 233 (1-4), pp. 275–287. DOI: 10.1016/j.apsusc.2004.03.229.
- Nolte, S.; Momma, C.; Jacobs, H.; Tünnermann, A.; Chichkov, B. N.; Wellegehausen, B.; Welling, H. (1997): Ablation of metals by ultrashort laser pulses. In *J. Opt. Soc. Am. B* 14 (10), p. 2716. DOI: 10.1364/JOSAB.14.002716.
- Severin Luzius, Marc Sailer, Jan Wieduwilt, Matthias Busch, Christof Siebert, Birgit Faisst (2012): Mikroproduktion im Laserfokus: Mikrobearbeitung mit UKP-Lasern. In *Scientific Reports Lasertechnik Photonik - IWKM* 2, pp. 44–47.
- Smarra, Marco; Dickmann, Klaus (2015a): Ultra-short pulse laser beam shaping for microstructuring using a deformable mirror. In *Laser Institute of America LIA (Ed.): ICALEO 2015, 34th International Congress on Applications of Lasers & Electro-Optics. Conference Proceedings : October 18-22, 2015. Atlanta, Ga., USA. ICALEO 2015. Atlanta, October 18-22, pp. 213–217.*
- Smarra, Marco; Dickmann, Klaus (2015b): Ultra-Short Pulse Laser Beam shaping for Microstructuring using a Deformable Mirror. In *Laser Institute of America LIA (Ed.): ICALEO 2015, 34th International Congress on Applications of Lasers & Electro-Optics. Conference Proceedings : October 18-22, 2015. Atlanta, Ga., USA. ICALEO 2015. Atlanta, October 18-22, pp. 213–216.*
- Smarra, Marco; Strube, Anja; Dickmann, Klaus (2016): Micro drilling using deformable mirror for beam shaping of ultra-short laser pulses. In Udo Klotzbach, Kunihiko Washio, Craig B. Arnold (Eds.): *SPIE LASE*. San Francisco, California, United States, Saturday 13 February 2016: SPIE (SPIE Proceedings), p. 97360.